Kovove Mater. 61 2023 267–275
DOI: 10.31577/km.2023.4.267

Comparison between spark plasma sintering and hot extrusion for solid-state recycling of Al-Si-Cu-Fe alloy chips

Ye Wang[1]*, Xiuyu Gao[1], Bo Jiang[1], Wentao Jiang[1], Dongdong Zhu[2], Maoliang Hu[1]

[1] *School of Materials Science and Chemical Engineering, Harbin University of Science and Technology, Harbin 150001, P. R. China*
[2] *Key Laboratory of Air-Driven Equipment Technology of Zhejiang Province, Quzhou University, Quzhou 324000, P. R. China*

Received 3 March 2023, received in revised form 28 March 2023, accepted 25 April 2023

Abstract

To investigate the low-cost and short-process recycling technologies for aluminium alloys, recycled chip-based Al-Si-Cu-Fe alloys were fabricated by spark plasma sintering (SPS) and hot extrusion. Microstructural observations by optical microscopy and scanning electron microscopy indicated that the recycled alloys could achieve good metallurgical bonding between the chips by fragmenting the alumina films on the chip surface by spark plasma sintering and hot extrusion after hot compress. The hot extruded recycled alloy has a smaller matrix grain size and second phase size than that of spark plasma sintered recycled alloys, due to the dynamic recrystallization and fragmentation of strong plastic deformation that occurs during the hot extrusion process. As a result, the chip-based Al-Si-Cu-Fe alloy recycled by hot extrusion after hot compress exhibited the best mechanical properties, with ultimate tensile strength, yield strength, and elongation of 258 and 132 MPa, and 8.6 % than that recycled by spark plasma sintering because of the effective metallurgical bonding between the chips, refinement of matrix grains, fragmentation and dispersion reinforcement of the oxide film and the second phase.

K e y w o r d s: Al-Si alloy, microstructure, mechanical properties, solid-state recycling, spark plasma sintering, hot extrusion

1. Introduction

As the most widely used lightweight alloy, aluminium alloys have high specific strength and good castability and corrosion resistance [1], in addition, when used as lightweight parts, aluminium alloys can also reduce energy consumption in transport, packaging, construction, and electrical conduction [2–5], especially in terms of CO_2 emissions [6]. However, with the extensive use of aluminium and its alloys, aluminium scrap generated during production and use gradually increases, so aluminium production currently must face sustainability limits [7]. Fortunately, as an infinitely recyclable metal [8–11], aluminium recycling can bring significant cost and environmental benefits [12], particularly through the solid-state recycling methods, which are usually considered to be a more suitable choice than remelting recycling due to the higher recycling rates [13, 14] and lower energy consumption and recycling costs [15]. Moreover, up to 90 % energy savings can even be achieved by an all-solid-state recycling process for aluminium alloys [16, 17].

The hot extrusion process and the spark plasma sintering (SPS) process are two common solid-state recycling processes. The hot extrusion process is often used to obtain finished or semi-finished products of recycled aluminium alloys [14, 18–20]. Tekkaya has recycled milled and turned AA6060 aluminium alloy chips by direct hot extrusion. The mechanical properties of the recycled alloy were equal to those of the as-cast alloy [21]. Haase also recycled the chips of AA6060 alloy through an integrated extrusion and equal channel angular pressing (iECAP) and suggested that the per-

*Corresponding author: e-mail address: wangye1984@hrbust.edu.cn

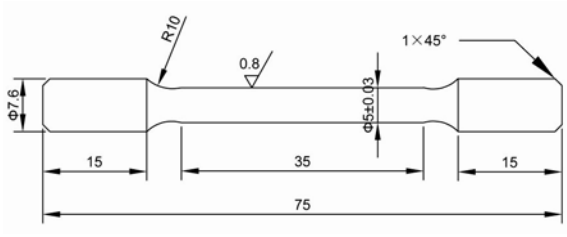

Fig. 1. The schematic diagram of the size of the tensile sample.

formance of the alloy recycled by the iECAP method was better than that of extruded as-cast alloy [22]. Güley improved the mechanical properties of the hot extruded AA6060 alloy recycled from machining chips by optimizing the design of the extrusion die based on the results of simulations and verification experiments [20].

As the most commonly used method in the field of powder metallurgy (PM), the Spark Plasma Sintering (SPS) process is able to metallurgical bonding of the metal chips or powders at low temperatures and short times, also with the advantage of low energy consumption [23]. Paraskevas recycled two different chips of AA6060 and AA8082 aluminium alloy by spark plasma sintering after cold pre-compaction and suggested that spark plasma sintering can be successful as one efficient solid-state recycling method to manufacture the near-net or even final shape products from the chips or turnings directly [24]. Li Bing recycled Mg-Gd-Y-Zn-Zr alloy by cold compact and spark plasma sintered chips to investigate the effect of SPS process parameters on the mechanical properties of the recycled alloy and reported that the oxide films at the bond interface between metal chips would be fragmented and hence obtained the superior bond properties between the chips [25].

Although both spark plasma sintering and hot extrusion are effective methods for recycling aluminium alloy from chips, the research on spark plasma sintering recycling of aluminium alloy chips and the comparison of the microstructures and mechanical properties of recycled alloys prepared by the two processes are rarely reported. Therefore, in this study, the milling chips of near-eutectic Al-Si-Cu-Fe alloy recycled by

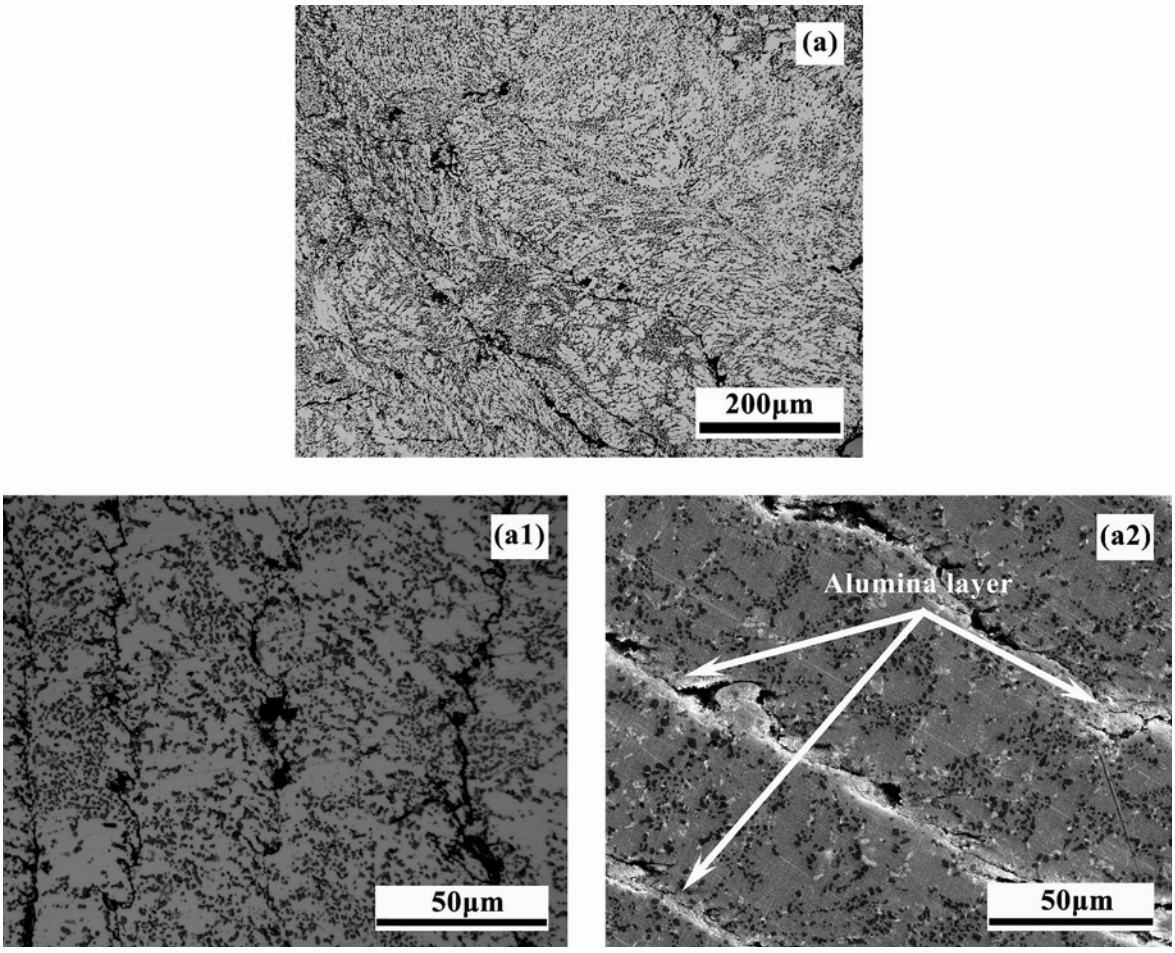

Fig. 2a. OM and SEM micrographs of the recycled alloys prepared by (a), (a1), and (a2) direct spark plasma sintering.

Table 1. Chemical composition in (wt.%) of the ADC12 alloys used for experiments [26]

Si	Cu	Fe	Mg	Zn	Mn	Ti	Al
10.56	1.91	0.85	0.21	0.55	0.28	0.03	Bal.

spark plasma sintering and hot extrusion were investigated. The effect of the two solid-state recycling methods on the microstructures and mechanical properties of recycled alloys was analyzed to obtain a recycling method with lower cost and better performance of the recycled alloy.

2. Experimental procedure

A typical die-casting Al-Si-Cu-Fe alloy, ADC12 alloy, was employed in this work, and the chemical composition is listed in Table 1. The chips of ADC12 alloy were prepared by milling the reducer bracket castings for automotive without any emulsion. The curled milling chips have a length of 4.3 ± 0.5 mm, 1.7 ± 0.3 mm width, and 0.3 ± 0.03 mm thickness. The solid-state recycling process of the chips was implemented in three ways: direct spark plasma sintering process, spark plasma sintering after hot compress, and hot extrusion after hot compress. During the hot compress process, chips were filled into a cylindrical H13 steel die 40 mm in diameter and then heated to 250 ℃ and pressed into a billet at a pressure of 640 MPa for 45 s. The spark plasma sintering was carried out on the LABOX-650F SPS apparatus, chips or billets were placed in the graphite die with a diameter of 40 mm, and then were heated to 450 ℃ with a heating rate of 60 ℃ min^{-1} at a vacuum of 50 Pa, and then held for 10 min under a uniaxial pressure of 40 MPa. The hot extrusion was performed in air at an extrusion temperature of 400 ℃ under the extrusion pressure of 864 MPa, and the extrusion ratio was 25 : 1.

The samples were ground, polished, and etched

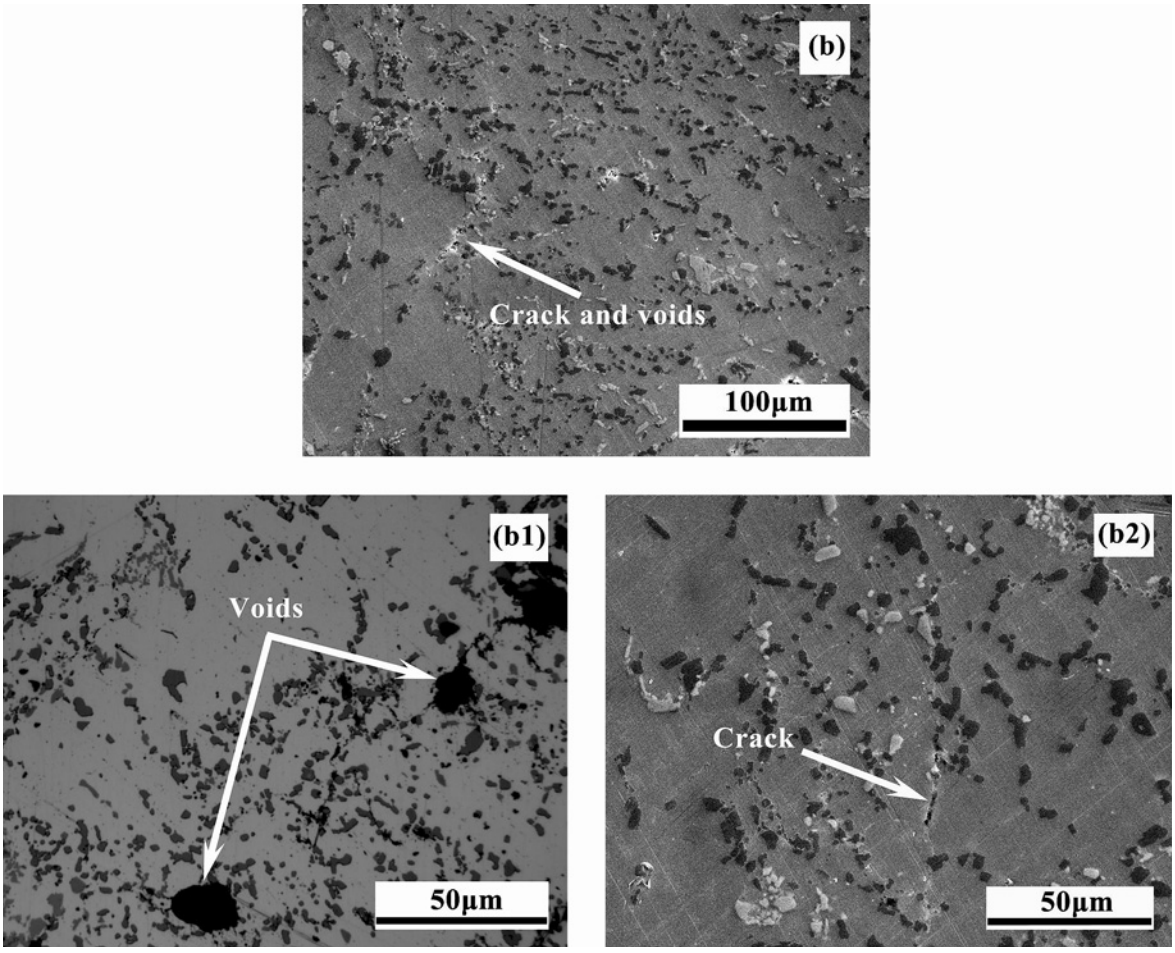

Fig. 2b. OM and SEM micrographs of the recycled alloys prepared by (b), (b1), and (b2) spark plasma sintering after hot compress.

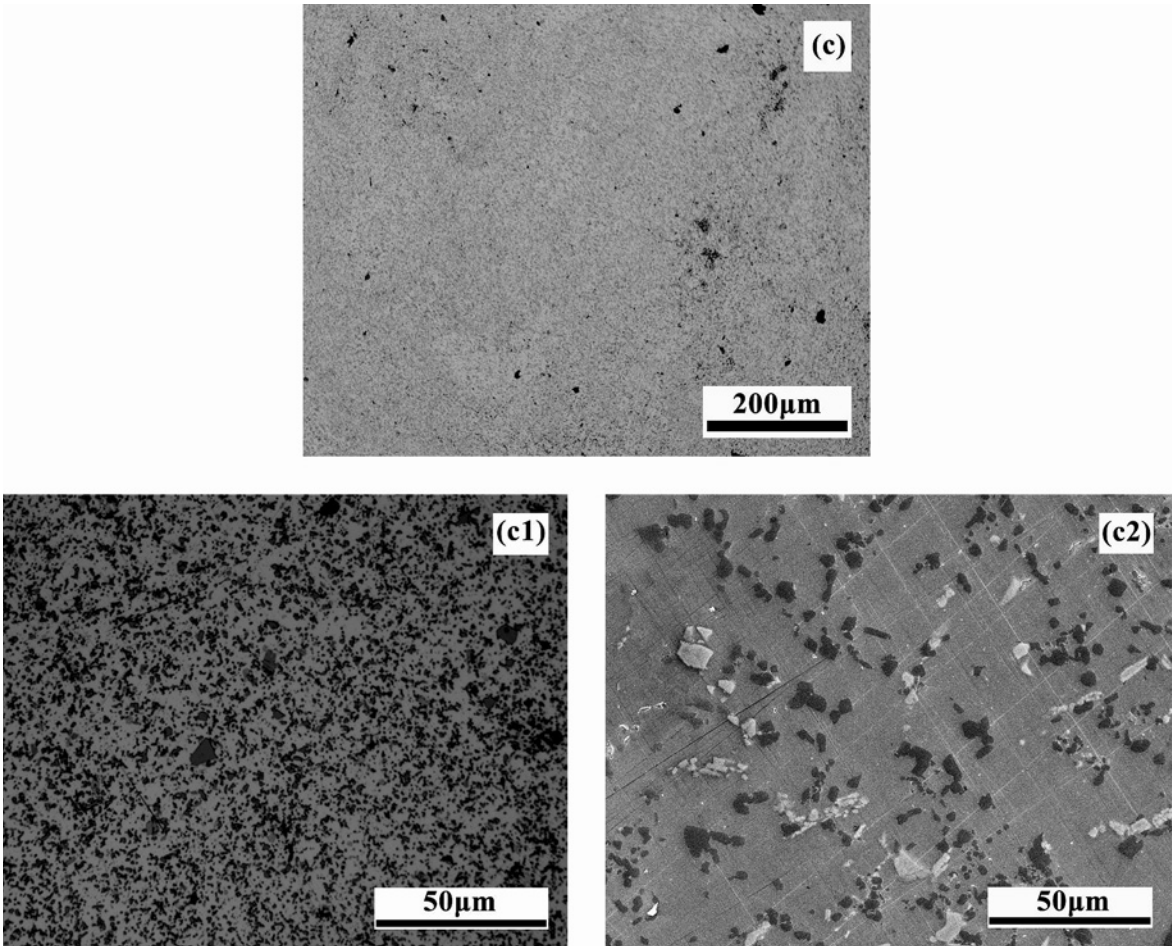

Fig. 2c. OM and SEM micrographs of the recycled alloys prepared by (c), (c1), and (c2) hot extrusion after hot compress.

with 1 % hydrofluoric acid (HF), then the microstructure observation was implemented by an optical microscope (OM) (Leica) and a scanning electron microscopy (SEM, Thermo scientific Apreo C) equipped with energy dispersive spectroscopy (EDS), which was also employed to characterize the fracture morphology of the alloys. Tensile tests were also performed by a universal material test machine (INSTRON 8861) at a constant strain rate of 1 mm min^{-1} at room temperature. And all of the specimens were machined into a 5 mm gauge diameter and 35 mm gauge length, as shown in Fig. 1, with the tensile axis parallel to the extrusion direction. Moreover, each specimen was measured at least five times, and then the average value was calculated for analysis.

3. Results and discussion

3.1. Microstructures

The optical microstructures of the recycling alloys prepared by the direct spark plasma sintering, spark plasma sintering, and hot extrusion after hot compress are shown in Fig. 2. It is obvious that extensive cracks and voids are present in the microstructure of the recycling alloys formed by direct spark plasma sintering, and the chips basically maintain the initial shape and are bonded together mainly in a mechanical manner with very low bond strength due to the hindered metallurgical bonding by the alumina layer on the surface of the chips, as shown by the bright white lines in Fig. 2a. The density of alloy recycled by spark plasma sintering after hot compress is much higher than that of the direct spark plasma sintered alloy because the alumina films at the bond interface can be fragmented during the hot compression process [25], the matrix surfaces can contact each other and achieve a good bond [15]. However, as marked in Figs. 2b,b1,b2, a few cracks and voids (larger than 20 μm in average size) are still present in the microstructure, indicating that the deformation provided by the hot compress has not achieved sufficient fragmentation of the alumina films on the chip surface. Furthermore, only a few small voids with a size of less than 5 μm can be observed in the alloy recycled by hot extrusion after hot compress, which reveals that the larger deformation can achieve effective metallurgical bonding between

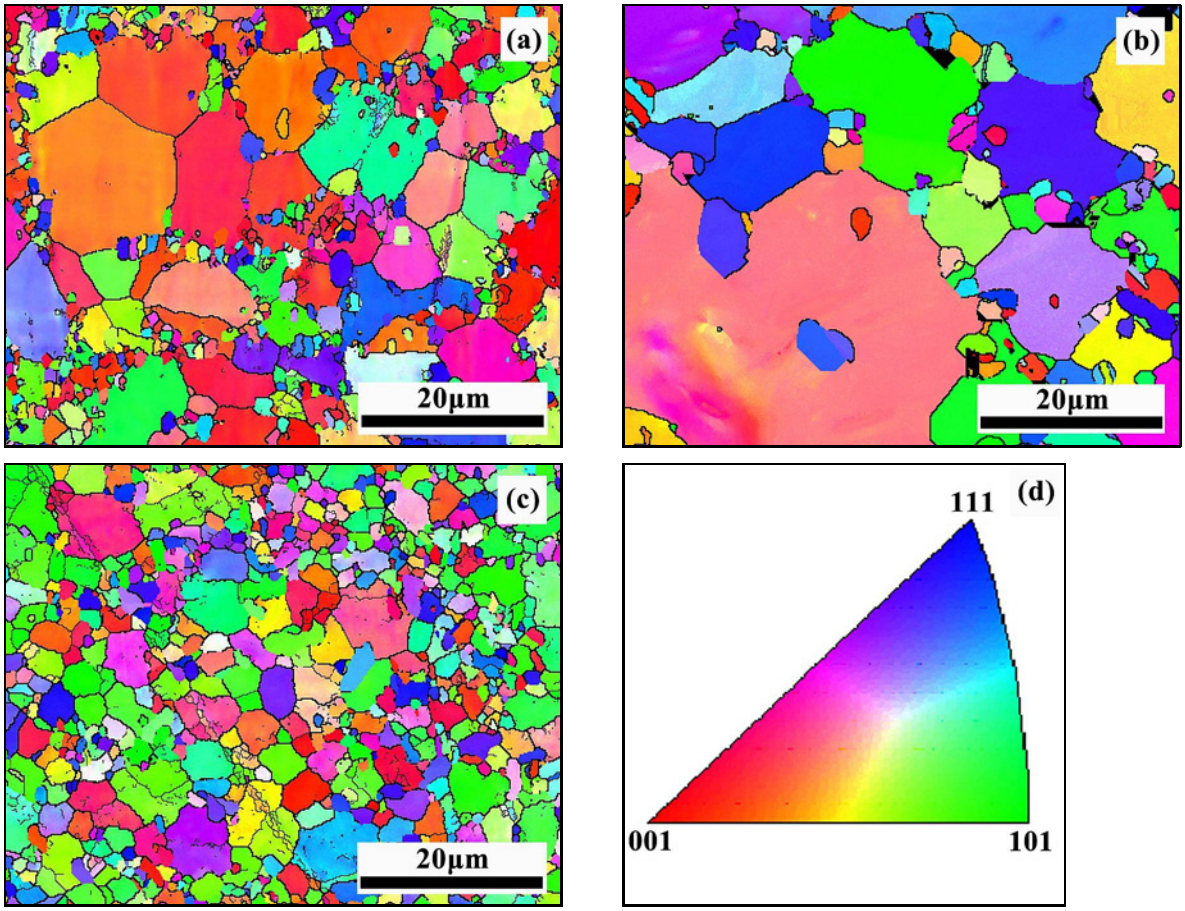

Fig. 3. Microstructures in IPF map of recycled alloys: (a) direct spark plasma sintering, (b) spark plasma sintering after hot compress, (c) hot extrusion after hot compress, and (d) legend.

the chips. Compared to the spark plasma sintered recycled alloys, as shown in Figs. 2a1,b2,c2, the hot extruded recycled alloy has a smaller second phase size due to the severe deformation provided by the milling and hot extrusion process, which further crushed the second phase particles, including β-Si phase and Fe-MICs, and reduced its size. Additionally, it is worth noting that neither of the recycling processes induced growth of the second phase.

To clearly illustrate the grain boundaries of the α-Al matrix, the inverse pole figure (IPF) map, recrystallization (RX) map, and the grain boundary (GB) map of the recycled alloys are shown in Figs. 3 and 4. It can be seen that many fine grains are distributed at the interface between the coarse grains due to the dynamic recovery and dynamic recrystallization that occurred during the direct spark plasma sintering process to relieve internal stresses induced by the milling process. The recrystallization (RX) results shown in Figs. 4a,c,e also indicate that the coarse grains were formed during dynamic recovery (yellow grains), and the fine grains were formed by dynamic recrystallization (blue grains) in the sintering process. In addition, some low-angle grain boundaries (LAGBs) (green lines) are still visible inside the deformed grains (red grains) in the GB map shown in Figs. 4b,d,f, indicating that dislocations introduced into the original grains by deformation during milling gradually develop into LAGBs during direct spark plasma sintering. But deformation from milling alone does not seem to be sufficient to promote dynamic recrystallization.

Compared with the microstructure of the direct spark plasma sintered recycled alloy, the grain size of recycled alloy prepared by spark plasma sintering after hot compress increased significantly, as shown in Figs. 4c,d. The RX and GB map results indicate that the dynamic recovery was facilitated by the hot compress and hence eliminating dislocations and LAGBs, while the coarse grains were formed by metallurgical bonding between chip interfaces during the subsequent sintering process. It is worth noting that the grains in the matrix of the alloy recycled by hot extrusion were obviously refined, as shown by the IPF map in Fig. 3c, due to the strong plastic deformation and dynamic recrystallization that occurred during hot extrusion [27]. At the same time, both the volume fraction of deformation grains (11 %) and LAGBs (26 %) increased, as shown in Figs. 4e,f. Thus, it can

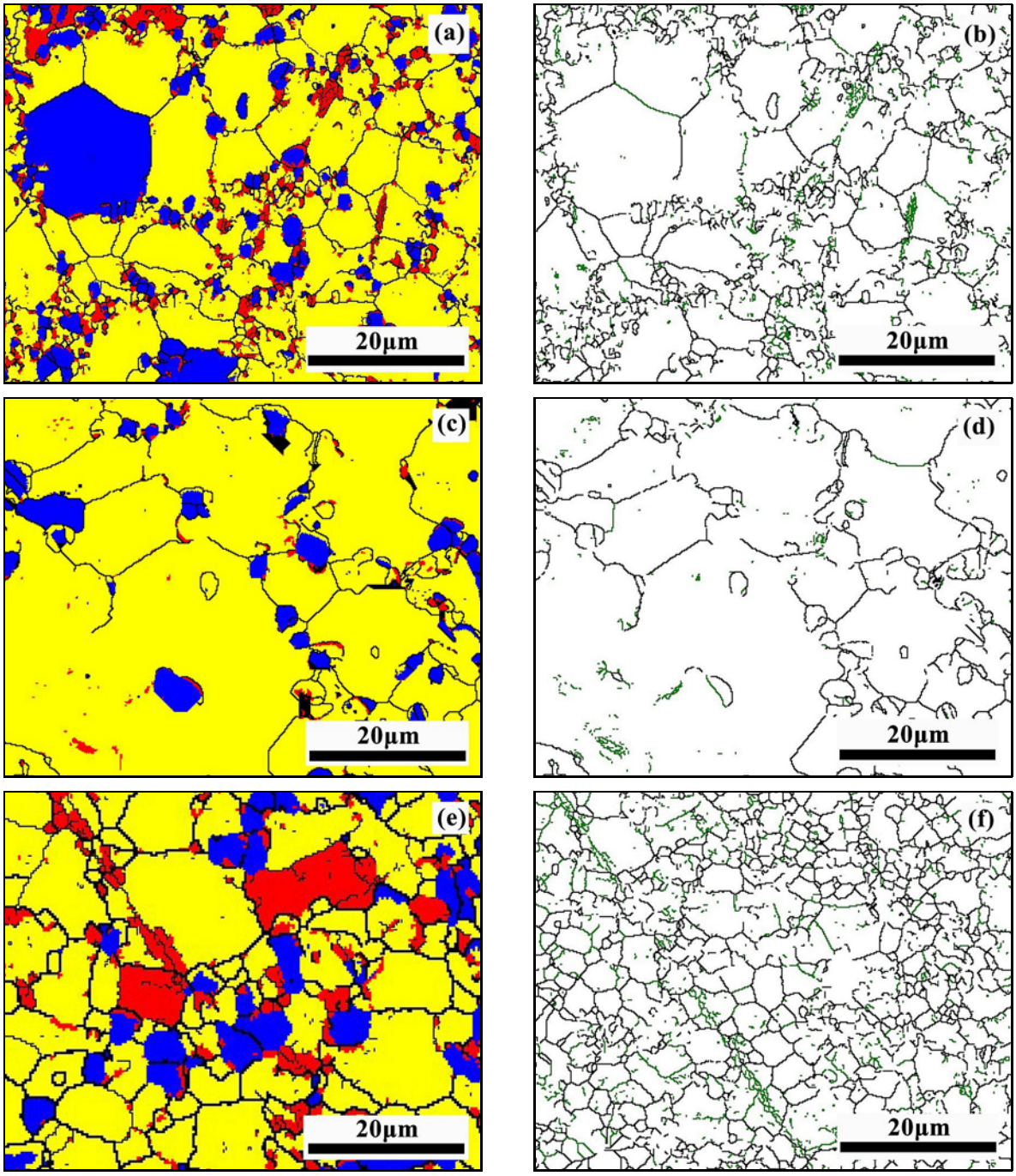

Fig. 4. Recrystallization (RX) map and grain boundary (GB) map of recycled alloys: (a), (b) direct spark plasma sintering, (c), (d) spark plasma sintering after hot compress, and (e), (f) hot extrusion after hot compress.

be deduced that hot extrusion not only fragmented the original grains and the second phase of the Al matrix but also effectively fragmented the alumina on the chip surface. During the transformation of LAGBs to HAGBs to form recrystallized grains, the broken and homogeneously distributed oxide prevented the further growth of dynamically recrystallized grains; thus, some fragmented grains developed into deformed grains with sub-structures in them.

3.2. Mechanical properties

Figure 5a plots the tensile properties of the recycled alloys prepared by different processes compared to the as-cast alloy. The ultimate tensile strength (UTS), yield strength (YS), and elongation of the direct spark plasma sintered recycled alloy are only 136 MPa, 88 MPa, and 3.3 %, respectively, which are lower than those of the as-cast alloy. However, the

mechanical properties of the alloy recycled after hot compress increased significantly, and the hot extrusion after hot compress recycled alloy exhibits the best mechanical properties with the UTS, YS, and elongation of 258 MPa, 132 MPa, and 8.6 %, respectively.

Obviously, the broken and dispersion reinforcement of the alumina and the effective metallurgical bonding between the chips during the hot extrusion effectively increases the strength of the alloy, while the milling process reduces the size of the second phase, including Si and Fe-MICs by fragmentation, which is particularly beneficial in increasing the elongation of the alloy. Figure 5 illustrates the fracture morphology of the recycled alloys using different processes. The fracture surfaces of the recycled alloy are all composed of small dimples, and the fracture surface of the recycled alloys prepared by direct spark plasma sintered recycled alloy and spark plasma sintered after hot compress shows a similar characteristic and dimple size. The large cracks that appeared in the fracture surface, as illustrated in Fig. 5c, verify the poor bonding between the chips during the direct spark plasma sintering. However, no cracks were observed at the fracture of both the alloys recycled by spark plasma sintering and hot extrusion after hot compress. Furthermore, the size of the dimples is like that of the second-phase particles revealing that the main fracture mechanism before the final damage of the recycled alloy is the cracking and debonding of these particles [28]. More and smaller dimples are observed in the fracture surface of the alloys recycled by hot extrusion from the refinement of the Al matrix and second phase, resulting in a significant improvement in the ductility of the alloy.

4. Conclusions

The microstructure and mechanical properties of the recycled ADC12 alloys from chips by direct spark plasma sintering, spark plasma sintering after hot compress, and hot extrusion after hot compress were investigated. The following conclusions are made:

1. The recycled alloys can achieve good metallurgical bonding between the chips by fragmenting the alumina films on the chip surface by spark plasma sintering and hot extrusion after hot compress. The hot extruded recycled alloy has a smaller size of matrix grain and second phase than that of spark plasma sintered recycled alloys, due to the dynamic recrystallization and fragmentation induced by strong plastic deformation that occurs during the extrusion process.

2. The best mechanical properties of the recycled alloy, with UTS, YS, and elongation of 258 MPa, 132 MPa, and 8.6 %, respectively, were obtained by hot extrusion after hot compress. The UTS, YS, and elongation of the direct spark plasma sintered recycled alloy are only 136 MPa, 88 MPa, and 3.3 %, respectively, due to the poor bonding between the chips hindered by the alumina layer on the surface of the chips.

3. The enhancement of the mechanical properties of the recycled alloys is mainly attributed to the effective metallurgical bonding between the chips, fragmentation, and dispersion strengthening of the alumina particles, and the second phase during the milling and hot extrusion process. Moreover, the diffuse distribution of alumina prevents the growth of dynamically recrystallized grains and thus refines the matrix grains, further improving the mechanical properties of the alloy recycled by hot extrusion after the hot compress process.

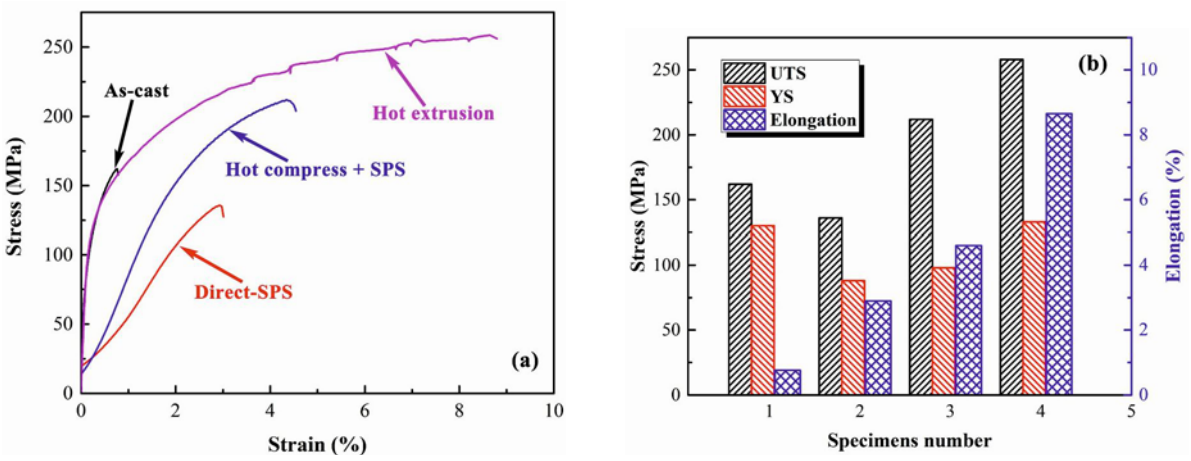

Fig. 5a,b. The tensile test results of (a) engineering stress-strain curves, (b) mechanical properties.

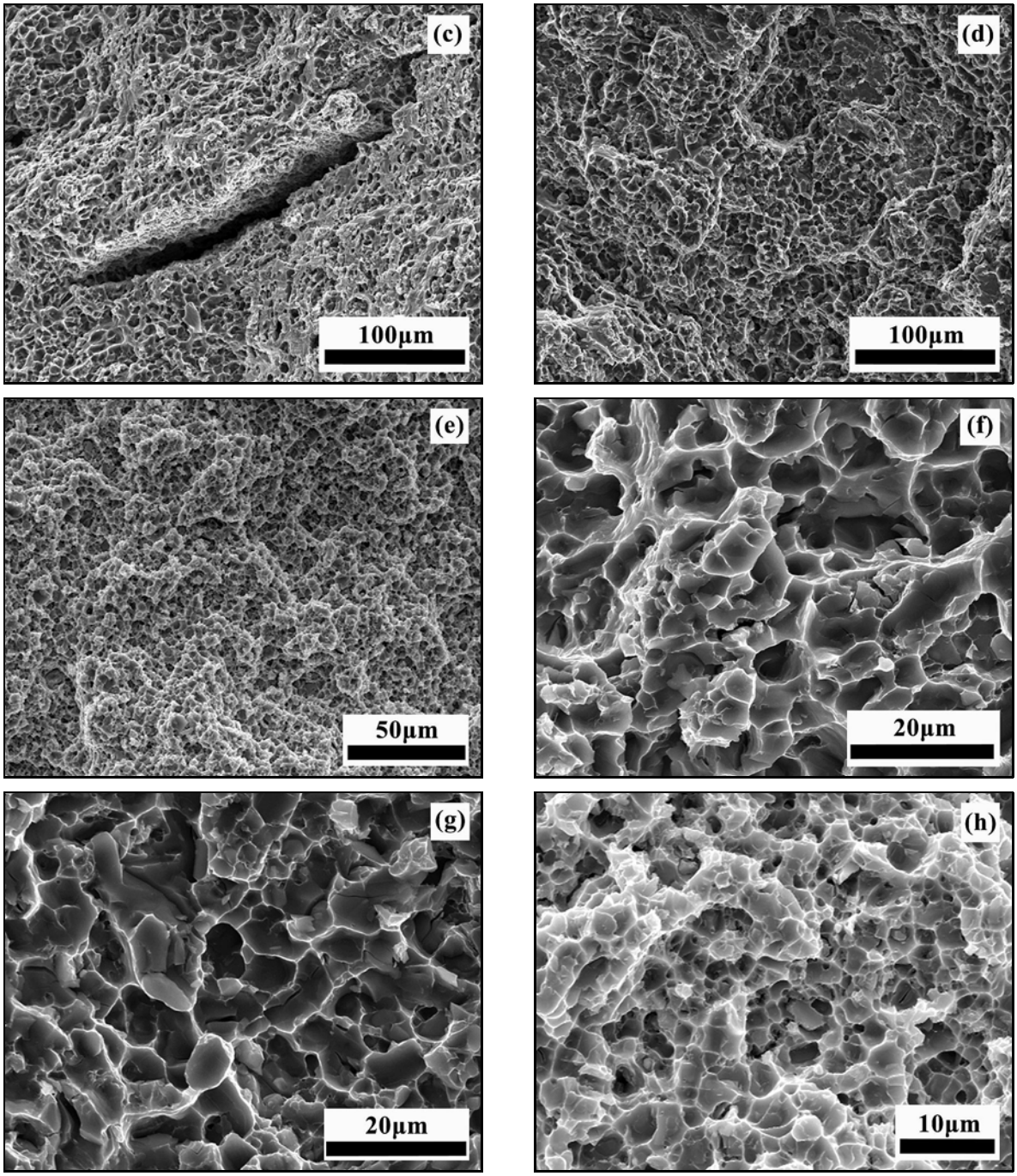

Fig. 5c–h. The tensile test results of the tensile fracture microstructures of recycled alloys in (c), (f) direct spark plasma sintering, (d), (g) spark plasma sintering after hot compress, and (e), (h) hot extrusion after hot compress conditions.

Acknowledgements

This work was supported by the National Natural Science Foundation of China (No. 52171113, 51801045).

References

[1] Z. H. Li, H. Yan, Z. Hu, X. C. Song, Fluidity of $ADC_{12} + x$La aluminum alloys, Rare Met. 40 (2021) 1191–1197. https://doi.org/10.1007/s12598-014-0383-3

[2] X. X. Meng, Y. X. Lin, Chip morphology and cutting temperature of ADC_{12} aluminum alloy during high-speed milling, Rare Met. 40 (2021) 1915–1923. https://doi.org/10.1007/s12598-020-01486-2

[3] S. Ford, M. Despeisse, Additive manufacturing and sustainability: an exploratory study of the advantages and challenges, J. Clean Prod. 137 (2016) 1573–1587. https://doi.org/10.1016/j.jclepro.2016.04.150

[4] M. K. Niaki, S. A. Torabi, F. Nonino, Why manufac-

turers adopt additive manufacturing technologies: The role of sustainability, J. Clean Prod. 222 (2019) 381–392. https://doi.org/10.1016/j.jclepro.2019.03.019
[5] N. T. Aboulkhair, M. Simonelli, L. Parry, I. Ashcroft, C. Tuck, R. Hague, 3D printing of aluminium alloys: Additive manufacturing of aluminium alloys using selective laser melting, Prog. Mater. Sci. 106 (2019) 100578. https://doi.org/10.1016/j.pmatsci.2019.100578
[6] M. S. Shahrom, A. R. Yusoff, M. A. Lajis, Taguchi method approach for recycling chip waste from machining aluminum (AA6061) using hot press forging process, Adv. Mater. Res. 845 (2014) 637–641. https://doi.org/10.4028/www.scientific.net/AMR.845.637
[7] D. Raabe, D. Ponge, P. J. Uggowitzer, M. Roscher, M. Paolantonio, C. L. Liu, H. Antrekowitsch, E. Kozeschnik, D. Seidmann, B. Gault, F. D. Geuser, A. Dechamps, C. Hutchinson, C. H. Liu, Z. M. Li, P. Prangnell, J. Robson, P. Shanthraj, S. Vakili, C. Sinclair, L. Bourgeois, S. Pogatscher, Making sustainable aluminum by recycling scrap: The science of "dirty" alloys, Prog. Mater. Sci. 128 (2022) 100947. https://doi.org/10.1016/j.pmatsci.2022.100947
[8] T. E. Graedel, J. Allwood, J. P. Birat, M. Buchert, C. Hagelüken, B. K. Reck, S. F. Sibley, G. Sonnemann, What do we know about metal recycling rates? J. Ind. Ecol. 15 (2011) 355–366. https://doi.org/10.1111/j.1530-9290.2011.00342.x
[9] T. E. Graedel, E. M. Harper, N. T. Nassar, B. K. Reck, On the materials basis of modern society, PNAS 112 (2013) 6295–6300. https://doi.org/10.1073/pnas.1312752110
[10] B. K. Reck, T. E. Graedel, Challenges in metal recycling, Science 337 (2012) 690–695. https://doi.org/10.1126/science.1217501
[11] J. B. Dahmus, T. G. Gutowski, What gets recycled: An information theory based model for product recycling, Environ. Sci. Technol. 41 (2007) 7543–7550. https://doi.org/10.1021/es062254b
[12] M. H. Rady, M. S. Mustapa, M. A. Harimon, M. R. Ibrahim, S. Shamsudin, M. A. Lajis, A. Wagiman, M. S. Msebawi, F. Yusof, Effect of hot extrusion parameters on microhardness and microstructure in direct recycling of aluminium chips, Materialwiss. Werkst. 50 (2019) 718–723. https://doi.org/10.1002/mawe.201800214
[13] J. M. Cullen, J. M. Allwood, Mapping the global flow of aluminum: From liquid aluminum to end-use goods, Environ. Sci. Technol. 47 (2013) 3057–3064. https://doi.org/10.1021/es304256s
[14] M. Haase, A. E. Tekkaya, Cold extrusion of hot extruded aluminum chips, J. Mater. Process. Tech. 217 (2015) 356–367. https://doi.org/10.1016/j.jmatprotec.2014.11.028
[15] B. B. Wan, W. P. Chen, T. W. Lu, F. F. Liu, Z. F. Jiang, M. D. Mao, Review of solid state recycling of aluminum chips, Resour. Conserv. Recy. 125 (2017) 37–47. https://doi.org/10.1016/j.resconrec.2017.06.004
[16] D. R. Cooper, J. M. Allwood, The influence of deformation conditions in solid-state aluminium welding processes on the resulting weld strength, J. Mater. Process. Tech. 214 (2014) 2576–2592. https://doi.org/10.1016/j.jmatprotec.2014.04.018
[17] V. Güley, K. N. Ben, A. E. Tekkaya, Direct recycling of 1050 aluminum alloy scrap material mixed with 6060 aluminum alloy chips by hot extrusion, Int. J. Mater. Form. 3 (2010) 853–856. https://doi.org/10.1007/s12289-010-0904-z
[18] M. Haase, A. E. Tekkaya, Recycling of aluminum chips by hot extrusion with subsequent cold extrusion, Procedia Engineering 81 (2014) 652–657. https://doi.org/10.1016/j.proeng.2014.10.055
[19] S. N. Ab Rahim, M. A. Lajis, S. Ariffin, A review on recycling aluminum chips by hot extrusion process, Procedia CIRP 26 (2015) 761–766. https://doi.org/10.1016/j.procir.2015.01.013
[20] V. Güley, A. Güzel, A. Jäger, N. B. Khalifa, A. E. Tekkaya, W. Z. Misiolek, Effect of die design on the welding quality during solid state recycling of AA6060 chips by hot extrusion, Mater. Sci. Eng. A 574 (2013) 163–175. https://doi.org/10.1016/j .msea.2013.03.010
[21] A. E. Tekkaya, M. Schikorra, D. Becker, D. Biermann, N. Hammer, K. Pantke, Hot profile extrusion of AA-6060 aluminum chips, J. Mater. Process. Tech. 209 (2009) 3343–3350. https://doi.org/10.1016/j.jmatprotec.2008.07.047
[22] M. Haase, N. B. Khalif, A. E. Tekkaya, W. Z. Misiolek, Improving mechanical properties of chip-based aluminum extrudates by integrated extrusion and equal channel angular pressing (iECAP), Mater. Sci. Eng. A 539 (2012) 194–204. https://doi.org/10.1016/j.msea.2012.01.081
[23] N. Kumar, A. Bharti, Review on powder metallurgy: A novel technique for recycling and foaming of aluminium-based materials, Powder Metall. Met. Ceram 60 (2021) 52–59. https://doi.org/10.1007/s11106-021-00214-4
[24] D. Paraskevas, K. Vanmeensel, J. Vleugels, W. Dewulf, Y. Deng, J. R. Duflou, Spark plasma sintering as a solid-state recycling technique: The case of aluminum alloy scrap consolidation, Materials 7 (2014) 5664–5687. https://doi.org/10.3390/ma7085664
[25] B. Li, B. Teng, Z. Zhu, Solid state recycling of Mg-Gd-Y-Zn-Zr alloy chips by spark plasma sintering, J. Magnes. Alloy 8 (2020) 1154–1165. https://doi.org/10.1016/j.jma.2019.09.014
[26] Y. Wang, H. Y. Xu, M. L. Hu, S. Sugiyama, Z. S. Ji, Enhanced mechanical properties of a chip-based Al-Si-Cu-Fe alloy with an in-situ emulsion decomposition recycled by solid-state processing, Results Phys. 12 (2019) 718–724. https://doi.org/10.1016/j.rinp.2018.12.036
[27] L. P. Zhong, J. Peng, M. Li, Y. J. Wang, Y. Lu, F. S. Pan, Effect of Ce addition on the microstructure, thermal conductivity and mechanical properties of Mg-0.5Mn alloys, J. Alloy Compd. 661 (2016) 402–410. https://doi.org/10.1016/j.jallcom.2015.11.107
[28] D. H. Kim, J. H. Kim, E. Kobayashi, Enhanced mechanical properties of Al-Si-Cu-Mg(-Fe) alloys by a deformation-semisolid extrusion process, Mater. Sci. Eng. A 825 (2021) 141667. https://doi.org/10.1016/j.msea.2021.141667